ACS chemical biology

Articles

pubs.acs.org/acschemicalbiology

An ABC Transporter with Two Periplasmic Binding Proteins Involved in Iron Acquisition in *Pseudomonas aeruginosa*

Karl Brillet,[†] Frank Ruffenach,[‡] Hendrik Adams,[†] Laure Journet,[†] Véronique Gasser,[†] Francoise Hoegy,[†] Laurent Guillon,[†] Mélissa Hannauer,[†] Adeline Page,[‡] and Isabelle J. Schalk*[,†]

[†]UMR 7242, Université de Strasbourg-CNRS, ESBS, Blvd Sébastien Brant, F-67412 Illkirch, Strasbourg, France

[‡]Institut de Génétique et de Biologie Moléculaire et Cellulaire (IGBMC), INSERM Unité 964/UMR 7104 CNRS, Université de Strasbourg, 1, rue Laurent Fries, 67404 Illkirch, France

Supporting Information

ABSTRACT: Pyoverdine I is the main siderophore secreted by *Pseudomonas aeruginosa* PAO1 to obtain access to iron. After extracellular iron chelation, pyoverdine-Fe uptake into the bacteria involves a specific outer-membrane transporter, FpvA. Iron is then released in the periplasm by a mechanism involving no siderophore modification but probably iron reduction. The proteins involved in this dissociation step are currently unknown. The pyoverdine locus contains the *fpvCDEF* operon, which contains four genes. These genes encode an ABC transporter of unknown function with the distinguishing characteristic of encompassing two periplasmic binding proteins, FpvC and FpvF, associated with the ATPase, FpvE, and the permease, FpvD. Deletion of these four genes partially inhibited cytoplasmic uptake of ^{55}Fe in the presence of pyoverdine and markedly slowed down the *in vivo* kinetics of iron release from the siderophore. This transporter is therefore involved in iron acquisition by pyoverdine in *P. aeruginosa*. Sequence alignments clearly showed that FpvC and FpvF belong to two different subgroups of periplasmic binding proteins. FpvC appears to be a metal-binding protein, whereas FpvF has homology with ferrisiderophore binding proteins. *In vivo* cross-linking assays and incubation of purified FpvC and FpvF proteins showed formation of complexes between both proteins. These complexes were able to bind *in vitro* PVDI-Fe, PVDI-Ga, or apo PVDI. This is the first example of an ABC transporter involved in iron acquisition *via* siderophores, with two periplasmic binding proteins interacting with the ferrisiderophore. The possible roles of FpvCDEF in iron uptake by the PVDI pathway are discussed.

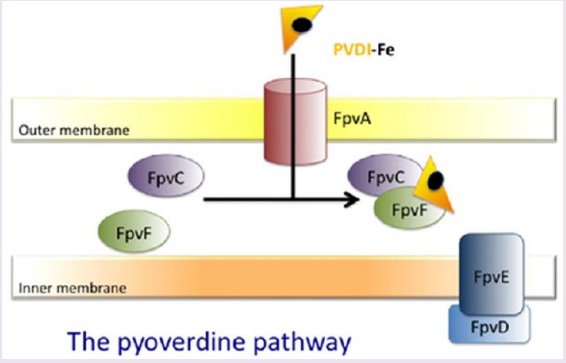

Under iron-deficient conditions, fluorescent *Pseudomonas* species are characterized by the overproduction and secretion of siderophores called pyoverdines.[1] Siderophores are high affinity iron chelators, which can solubilize iron and deliver it into the bacterial cells.[2] They are important for the survival and growth of bacteria in soil and aqueous environments. Siderophores also underlie the virulence of many pathogens in animal models of disease where they compete with the host's iron-chelating proteins such as transferrin or lactoferrin.[3] Over 60 pyoverdines have been identified,[4] forming a large class of siderophores characterized by a conserved dihydroxyquinoline-derived chromophore to which a peptide chain of variable length and composition is attached. The size and amino-acid composition of the peptide moiety of pyoverdines are unique to each *Pseudomonas* species, indicating that the specialization of each bacterium is determined by its siderophore. *Pseudomonas aeruginosa* PAO1 produces the siderophore pyoverdine I (PVDI), a partly cyclic octapeptide linked to the chromophore.[5] Among *Pseudomonas*, biosynthesis of pyoverdine and iron uptake mechanisms are the best known for PVDI in *P. aeruginosa* PAO1. In parallel to PVDI, *P. aeruginosa* is able to produce and use the siderophore pyochelin (PCH) and is able to use siderophores produced by other microorganisms, such as ferrichrome, enterobactine, and cepabactin.[6]

After chelation of iron in the extracellular medium, PVDI-Fe is transported across the *P. aeruginosa* outer membrane by FpvAI, which is a specific outer-membrane transporter. FpvAI consists of a C-terminal β-barrel domain, a plug domain filling the barrel, followed by a region of four to five residues called the TonB box, and a long periplasmic N-terminal extension.[7,8] This extension is not involved in the transport of ferrisiderophores but functions in the regulation of transcription *via* a signaling cascade.[9] The binding site of the ferric siderophore is located outside the membrane above the plug and is composed of residues from both the plug and the β-barrel domains. The FpvAI binding site mostly consists of aromatic residues, including six Tyr residues and two Trp residues, and only three hydrophilic residues. As in all Gram-negative bacteria, the proton-motive force of the inner membrane drives the transport of ferrisiderophore across the outer membrane through

Received: July 5, 2012
Accepted: September 25, 2012
Published: September 25, 2012

interaction of the inner-membrane TonB protein with the TonB box of the outer-membrane transporter.[10,11]

In Gram-negative bacteria, the subsequent uptake of ferrisiderophores across the inner membrane is performed by either a transporter, belonging to the family of periplasmic binding protein-dependent ABC transporters,[12] or by permeases.[13,14] In *Escherichia coli*, the transport of ferric siderophores is sustained by a specific ABC transporter for each siderophore pathway: FhuBCD for desferrichrome and desferrioxamine,[15,16] FecCDE for citrate,[17,18] and FepCDG for enterobactin.[19] In *P. aeruginosa*, ferripyochelin and ferrichrome are transported across the inner membranes by permeases: FptX for ferripyochelin,[13] and FiuB and FoxB for ferrichrome.[14] For these siderophore pathways, the whole ferrisiderophore complex is transported into the cytoplasm and iron is then released from the siderophore. The release mechanisms for ferrichrome involve iron reduction[20] followed by acetylation of the siderophore and its recycling into the growth media.[14,21] The release mechanism for ferrienterobactin involves cytoplasmic esterase hydrolysis of the siderophore.[22] Previous studies indicated that the dissociation of the PVDI-Fe complex occurs in the periplasm and not in the cytoplasm.[23,24] This process does not involve any chemical degradation or modification of the siderophore, but apparently an iron reduction. PVDI is then recycled to the extracellular medium by the PvdRT-OpmQ efflux pump[24−26] thereby allowing a new cycle of iron uptake to take place. However, the molecular mechanisms involved in the release of metal from PVDI and the reuptake of iron from the periplasm to the cytoplasm remain unknown.

In *P. aeruginosa* PAO1, a periplasmic binding protein-dependent ABC transporter is present at the pyoverdine locus (PA2407-10) and conserved in most *Pseudomonas* species apart in the non-fluorescent *Pseudomonas stutzeri* and *Pseudomonas mendocina*.[27] Expression of these genes is regulated by iron, PvdS,[27−29] and two other ECF factors.[28] Mutation of PA2407-10 genes does not appear to affect growth or PVDI production under iron-limiting conditions,[30] another iron uptake pathway probably taking over this process. According to its genome, *P. aeruginosa* PAO1 has at least 11 iron uptake pathways.[31] In the present study, we reinvestigated the involvement of PA2407-10 genes in iron acquisition *via* the PVDI pathway in *P. aeruginosa* PAO1. We showed that deletion of these four genes affects cytoplasmic ^{55}Fe acquisition *via* PVDI and inhibited the kinetics of iron release from this siderophore in bacterial cells. *In vitro* experiments with purified FpvC and FpvF (the two periplasmic binding proteins of this ABC transporter) and *in vivo* cross-linking experiments showed formation of complexes with different stochiometries for the FpvC and FpvF proteins. These complexes could bind PVDI-Fe and apo PVD.

RESULTS AND DISCUSSION

fpvCDEF Are Predicted To Encode an ABC Transporter. The sequence of PA2407-10, called here *fpvCDEF* and which is located in the *pvd* locus,[27,28] is predicted to form an operon encoding a periplasmic binding protein dependent ABC transporter. PA2408 (*fpvD*) codes for a probable ATP-binding component, and PA2409 (*fpvE*) encodes a probable permease of an ABC transporter. PA2407 (*fpvC*) and PA2410 (*fpvF*) are predicted to encode proteins of the TroA-like superfamily.[32] Such proteins are periplasmic binding components of ABC-type transport systems that bind ferric siderophores and metal ions such as Mn^{2+}, Fe^{3+}, Cu^{2+}, and/or Zn^{2+}. These proteins have a similar organization; two independent globular domains interact with each other to create the binding cleft between them.[33] TroA-like proteins are generally encoded by ABC-type operons such as *fpvCDEF*. A 317-amino-acid periplasmic protein of 34309.4 Da is expected from the nucleotide sequence of FpvC (PA2407) (http://www.expasy.ch/cgi-bin/protparam). A signal sequence is predicted by SignalP,[34] with a putative cleavage site between residues 37 and 38. From the expected final amino-acid sequence, the predicted molecular mass of the mature form of the FpvC protein is 30457.7 Da.

The nucleotide sequence for FpvF (PA2410) predicts a 305-amino-acid periplasmic protein. SignalP predicted a putative cleavage site between residues 25 and 26,[34] and the expected molecular mass of the mature protein is 30143.3 Da. The molecular weight of each protein was confirmed by ESI-MS analysis under denaturing conditions on purified FpvC and FpvF. The experimental values obtained after deconvolution of the multicharged spectra are 30457 Da for FpvC and 30145 Da for FpvF (Supplemental Table 1). Under native conditions, the molecular weight observed for FpvC was 30522 Da. This higher medium molecular weight corresponded to the addition of three sodium adducts.

Amino-acid sequence alignments clearly indicated that FpvC and FpvF belong to two different subgroups of TroA-like proteins (Figure 1). The first group includes FpvC, TroA, ZnuA, and MntA and corresponds to metal-binding proteins. The second group is composed of FpvF, BhuT, and FhuD, which are all proteins involved in ferrisiderophore binding. For FpvC (as for TroA, ZnuA, and MntA), the four amino-acid residues involved in metal chelation (three His and one Asp) are conserved, suggesting that FpvC is able to chelate a metal. The sequence alignment for FpvF suggests that this protein has a role in ferrisiderophore binding like FhuD and BhuT (Figure 1). For these proteins, the binding site recognizes the siderophore but not the chelated metal.[35] On the basis of these sequence homologies, FpvCDEF appears to be a mixed ABC transporter that can interact with both a siderophore and a metal *via* its two periplasmic binding proteins.

FpvCDEF Deletion Partially Affects ^{55}Fe Uptake by PVDI and Cytoplasmic ^{55}Fe Accumulation. We assessed the ability of a mutant with a *fpvCDEF* deletion to transport and accumulate ^{55}Fe in the presence of PVDI. To avoid iron uptake by the siderophore pyochelin (PCH) and in order to control the concentration of PVDI in the experiments, the PCH- and PVDI-negative *P. aeruginosa* mutant PAO6383 (Table 1) and its *fpvCDEF* deletion mutant derivative PAS158 were used. Bacteria were incubated with two different PVDI-^{55}Fe concentrations, 100 and 500 nM, and the radioactivity incorporated into the cells was monitored (Figure 2). For 500 nM PVDI-^{55}Fe, around 30% inhibition of iron uptake was observed for the *fpvCDEF* mutant. When PAS158 was complemented with pMH3L, a pMMB derivative carrying the *fpvCDEF* genes, this iron uptake was restored to the level measured for PAO6383. Accordingly, FpvC and FpvF are highly expressed in these complemented cells (Supplemental Figure 1). PVDI-^{55}Fe uptake inhibition was never complete, even with increasing PVDI-^{55}Fe concentrations (1 μM, data not shown). In the presence of 100 nM PVDI-^{55}Fe, no iron uptake inhibition was observed, probably because the concentration is not high enough and would only allow one or two turnovers of FpvA transport. We repeated the experiment for each strain after treating the cells with the protonophore CCCP. This compound inhibits the proton motive force (PMF) of the bacteria and thus also inhibits any TonB-dependent uptake.[36] As expected, no

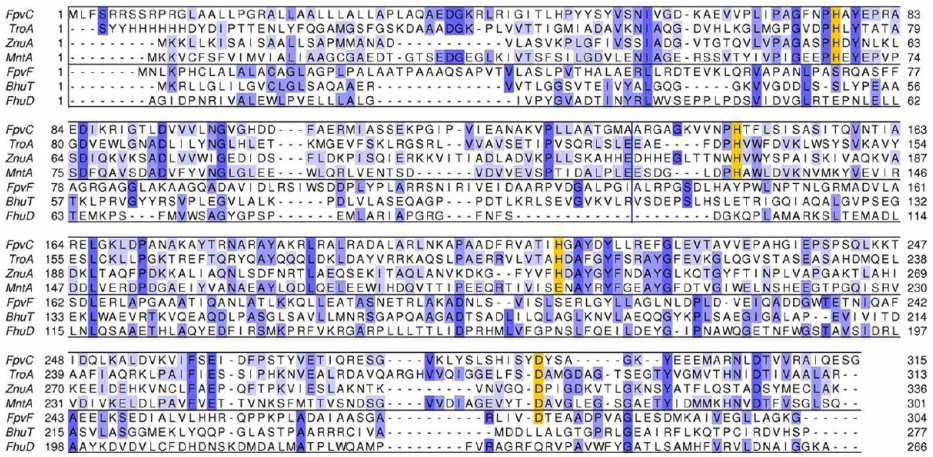

Figure 1. Sequence alignment of FpvC (PA2407) and FpvF (PA2410) with proteins belonging to the TroA superfamily, shown to function in the ABC transport of ferric siderophores and metal ions such as Mn^{2+}, Fe^{3+}, Cu^{2+}, and/or Zn^{2+}. Invariant residues as well as highly conserved residues are shaded in blue. Residues occupying conserved positions but deviating from the consensus amino-acid sequence are shaded in brighter blue. The four residues of TroA involved in metal chelation are shaded in yellow. The blue vertical line indicates a 44 amino-acid extension of ZnuA, which is not represented on the alignment. Sequence alignment was performed using CLUSTALW [52] and was manually readjusted by accounting for the residues involved in metal chelation. Two subgroups are shown. The upper group, composed of FpvC, TroA, ZnuA and MntA, corresponds to metal-binding proteins whereas the lower group, composed of FpvF, BhuT, and FhuD, contains proteins involved in ferrisiderophore chelation.

Table 1. Strains and Plasmids Used in This Study

strains or plasmids	relevant characteristics	source or reference
	P. aeruginosa Strains	
PAO1	wild-type strain	46
PAO6383	derivative of PAO1; Δ*pvdF* Δ*pchBA*	47
PAS158	derivative of PAO1; Δ*pvdF* Δ*pchBA* Δ*fpvCDEF*	this study
PAO*pvdFfpvA*	derivative of PAO1; *pvdF*::kana, Δ*fpvA*	48
PAO*fpvC*	derivative of PAO1; pvdC::Gm^R	30
	E. coli Strains	
TOP10	F$^-$, *mcrA* Δ(*mrr-hsdRMS-mcrBC*) Φ80*lacZ*Δ*M15* Δ*lacX74 recA1 araD139* Δ(*ara-leu*)*7697 galU galK rpsL endA1 nupG*	Invitrogen
BL21(DE3)	*F– ompT hsdS*$_B$(r_B –m_B –) *gal dcm* (λ DE3)	Novagen
	Plasmids	
pMMB190	Amp^R, RSF replicon (*Inc.Q*), *tac* promoter	49
pME3088	suicide vector; Tc^R ; ColE1 replicon ; *Eco*RI *Kpn*I *Dra*II *Xho*I *Hin*dIII polylinker	50, 51
pME497	mobilizing plasmid, ApR	51
pJET1/blunt vector	rep (pMB1), *bla* (Ap^R), *eco47IR*, PlacUV5	Fermentas
pMH3L	pMMB190 carrying *Bam*HI-*Hin*dIII fragment containing *fpvCDEF*	this study
pLJ68	pJET1/blunt carrying *Eco*RI-*HindIII* fragment containing the 700bp upstream *fpvC* and the 700 pb downstream *fpvF*.	this study
pLJ76	pME3088 carrying *Eco*RI-*HindIII* fragment containing the 700bp upstream *fpvC* and the 700 pb downstream *fpvF*.	this study
pET23–789	pET23 carrying a fragment containing the *fpvCDE* genes	this study
pVEGA6	pMMB190 carrying *Eco*RI-*Hin*dIII fragment containing *fpvF*-6His	this study

iron uptake occurred with CCCP-treated cells (Figure 2). The inhibition of ^{55}Fe accumulation in cells that are unable to express the FpvCDEF ABC transporter indicates a role of FpvCDEF in the uptake of iron *via* the PVDI pathway.

The uptake experiments in the presence of 500 nM PVDI-^{55}Fe were repeated, and cells were fractionated after 30 min of incubation with the siderophore-iron complex and radioactivity in each cell compartment was monitored (Figure 2C). Around 45% less radioactivity was detected in the cytoplasm of PAS158 compared to that of PAO6383. The amount of ^{55}Fe in the periplasm seemed to be independent of the FpvCDEF expression. In the complemented strain PAS158(pMH3L) the amount of ^{55}Fe increased in both periplasm and cytoplasm, consistent with the high expression of the FpvCDEF proteins in this strain (Supplemental Figure 1).

All of these observations indicate that the ABC transporter FpvCDEF is involved in the uptake of iron by the siderophore PVDI and plays a role in iron translocation from the periplasm into the cytoplasm. In the absence of FpvCDEF, PVDI-^{55}Fe can still be transported across the outer membrane by FpvA but accumulates into the periplasm. This periplasmic ^{55}Fe accumulation explains why in *fpvCDEF* mutant PAS158 only 30% inhibition of ^{55}Fe uptake is observed.

fpvCDEF Deletion Affects PVDI-Fe Dissociation *in Vivo*. Previous studies have shown that iron is released from PVDI in the periplasm through a mechanism probably involving iron reduction.[23,24] This dissociation can be followed in real time by exciting the bacterial sample at 400 nm and monitoring the fluorescence at 447 nm.[23] Only apo PVDI is fluorescent at 447 nm (excited at 400 nm[37,38]). In its ferric form, iron quenches the fluorescence of the siderophore. To investigate further the role of FpvCDEF in iron uptake by PVDI in *P. aeruginosa*, cells of the PVDI-negative mutant PAO6383, its *fpvCDEF* mutant PAS158, the corresponding complemented strain PAS158(pMH3L), and the *fpvA* mutant PAO*pvdFfpvA* were incubated in the presence 20 nM or 100 nM PVDI-Fe (Figure 3). Consistent with previous findings,[23] an increase in fluorescence was observed following the addition of PVDI-Fe to PAO6383. This corresponded to the dissociation of PVDI-Fe (formation of fluorescent apo PVDI) in the bacterial periplasm. No increase of fluorescence was observed in the absence of FpvA, where no PVDI-Fe can be transported into the bacteria. For both tested ferrisiderophore concentrations, deletion of the *fpvCDEF* genes resulted in a clear decrease of the kinetics of PVDI-Fe dissociation (0.034 and 0.356 ΔF min^{-1} for PAS158 and

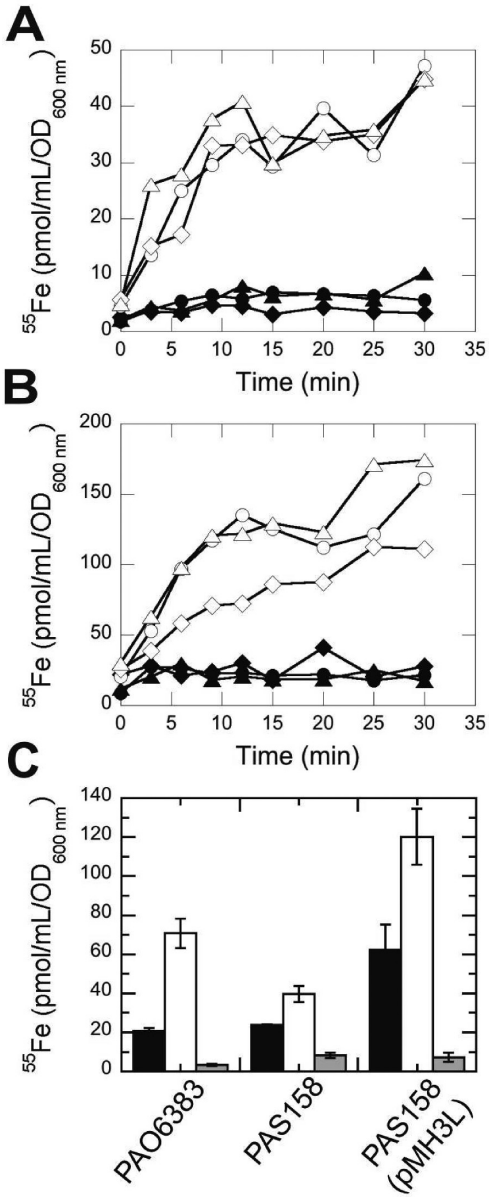

Figure 2. (A, B) Time-dependent uptake of PVDI-^{55}Fe in *P. aeruginosa* PAO6383, PAS158, and PAS158(pMH3L) strains. PAO6383 is a PCH- and PVDI-negative strain, PAS158 its *fpvCDEF* deletion mutant, and PAS158(pMH3L) the complemented *fpvCDEF* strain. Cells were incubated for 15 min in 50 mM Tris-HCl (pH 8.0) before the initiation of transport assays by the addition of 100 (panel A) or 500 (panel B) nM PVD-^{55}Fe (PAO6383, ○; PAS158, ◇; and PAS158(pMH3L), Δ). Samples (100 μL) from the suspension were removed at various time points and filtered; the radioactivity retained was measured. The results are expressed as pmol of PVD-^{55}Fe transported per mL of cells at an OD$_{600\ nm}$ of 1. The experiment was repeated with the CCCP protonophore at a concentration of 200 μM (PAO6383, ●; PAS158, ◆; and PAS158(pMH3L), ▲). The experiments were repeated three times, and equivalent kinetics were observed. (C) ^{55}Fe repartition in the different cell compartments of *P. aeruginosa* cells. PAO6383, PAS158, and PAS158(pMH3L) cells were incubated for 30 min in the presence of 500 nM PVDI-^{55}Fe in the same condition as for the uptake assays in panel B. Afterward, the cells were pelleted, the periplasms (black bars), cytoplasms (white bars), and membranes (gray bars) were isolated for each strain, and the amount of ^{55}Fe present was monitored.

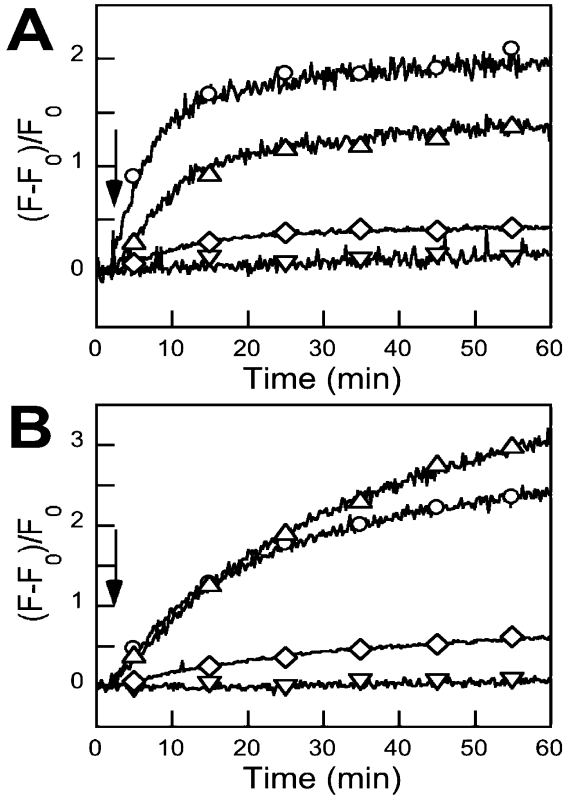

Figure 3. *In vivo* PVD-Fe dissociation kinetics, monitored by direct excitation of PVD in PAO6383 (○), PAS158 (◇), PAS158(pMH3L) (Δ), and PAO*pvdFfpvA* (▽) cells. PAO6383 is a PCH- and PVDI-negative strain, PAS158 its *fpvCDEF* deletion mutant, PAS158-(pMH3L) the complemented *fpvCDEF* strain, and PAO*pvdFfpvA* a PVDI- and FpvA mutant. Cells were washed and resuspended to an OD$_{600\ nm}$ of 0.2 in 50 mM Tris-HCl pH 8.0 and incubated at 29 °C. Following the addition of 20 (panel A) or 100 nM (panel B) PVDI-Fe (indicated by an arrow), the change in fluorescence (excitation set at 400 nm) was monitored by measuring the emission of fluorescence at 447 nm, every second, for 60 min. The experiments wererepeated three times, and equivalent kinetics were observed.

PAO6383, respectively) in the presence of 100 nM PVDI-Fe as compared to the PAO6383 mutant (Figure 3B), and around 85% less apo PVDI was generated. The experiment was also carried out with PAS158 cells carrying pMH3L. Dissociation was restored in PAS158 cells complemented with the four *fpvCDEF* genes (Figure 3).

In conclusion, the data presented in Figures 2 and 3 suggest that FpvCDEF must be involved in the transport of iron across the inner membrane and that this transporter is necessary for an efficient PVDI-Fe dissociation. Previous studies have shown that iron is apparently removed from PVDI in the periplasm by a mechanism involving iron reduction and no degradation of the siderophore[23−26] and that PVDI is able to bind and oxidize the ferrous ion *in vitro*.[39] Therefore, FpvCDEF, by exporting iron across the inner membranes, may activate PVDI-Fe dissociation.

FpvF Interacts More Efficiently with PVDI-Fe than FpvC. FpvC was overexpressed in *E. coli*, and FpvF was over-expressed in *P. aeruginosa* cells. After their purification, both proteins were analyzed independently by ESI-MS. This technique has become widely used for primary-structure determination and characterization of purified proteins. It has also been used to assess the stability of noncovalent complexes in the vacuum of

dx.doi.org/10.1021/cb300330v | *ACS Chem. Biol.* 2012, 7, 2036−2045

Table 2. Complexes Formed between FpvC, FpvF and PVDI, PVDI-Fe, and Siderophore-Free Fe^{3+} [a]

proteins incubated with or without siderophores	proteins or complexes observed and experimental molecular weight in native condition (Da)
FpvC	FpvC: 30522 (+3 Na^+)
FpvC + Fe^{3+}	no FpvC-Fe complex was observed
	FpvC: 30 522
FpvC + PVDI	FpvC-PVDI: 31856
	FpvC
FpvC + PVDI-Fe	FpvC-PVDI-Fe
	(masses presented in Figure 4A)
FpvF	FpvF: 30145
	$FpvF_2$: 60291
FpvF + Fe^{3+}	no FpvF-Fe or $FpvF_2$-Fe complexes were observed
	FpvF
FpvF + PVDI	$FpvF_2$
	$FpvF_2$-PVDI
	(masses presented in Figure 4B)
	FpvF
FpvF + PVDI-Fe	$FpvF_2$
	$FpvF_2$-PVDI-Fe
	(masses presented in Figure 4C)
FpvC + FpvF	FpvC
	FpvF
	$FpvF_2$
	FpvC-$FpvF_2$
	$FpvC_2$-$FpvF_2$
	(masses presented in Figure 5)
FpvC + FpvF + Fe^{3+}	FpvC
	FpvF
	FpvC-$FpvF_2$
	$FpvC_2$-$FpvF_2$
FpvC + FpvF + PVDI	FpvC
	FpvF
	FpvC-PVDI
	FpvC-$FpvF_2$
	FpvC-$FpvF_2$-PVDI
	FpvC-$FpvF_2$-$PVDI_2$
	$FpvC_2$-$FpvF_2$
	$FpvC_2$-$FpvF_2$-PVDI
	$FpvC_2$-$FpvF_2$-$PVDI_2$
	(masses presented in Figure 7A)
FpvC + FpvF + PVDI-Fe	FpvC
	FpvF
	FpvC-PVDI-Fe
	FpvC-$FpvF_2$
	FpvC-$FpvF_2$-PVDI-Fe
	FpvC-$FpvF_2$-$PVDI_2$−Fe_2
	$FpvC_2$-$FpvF_2$
	$FpvC_2$-$FpvF_2$-PVDI-Fe
	$FpvC_2$-$FpvF_2$-$PVDI_2$−Fe_2
	(masses presented in Figure 7B)
FpvC + FpvF + PVDI-Ga	FpvC
	FpvF
	FpvC-PVDI-Ga
	FpvF-PVDI-Ga
	$FpvF_2$
	$FpvF_2$-PVDI-Ga
	FpvC-$FpvF_2$
	FpvC-$FpvF_2$-PVDI-Ga
	FpvC-$FpvF_2$-$PVDI_2$-Ga_2
	$FpvC_2$-$FpvF_2$
	$FpvC_2$-$FpvF_2$-PVDI-Ga
	$FpvC_2$-$FpvF_2$-$PVDI_2$-Ga_2
	(masses presented in Supporting Information)

[a]FpvC and FpvF were incubated independently or together, in the presence or in the absence of 10 equiv of PVDI, PVDI-Fe, or $FeCl_3$ in 100 mM ammonium acetate pH 6.5 buffer. The analyses of samples by ESI-MS were realized under native conditions with a final concentration of 10 pmol/μL FpvC and FpvF in 150 mM ammonium acetate. The experimental molecular weights correspond to the molecular weights obtained after the deconvolution of the multicharged ions in native conditions, and the composition of the complexes formed was deduced from the molecular weight.

the mass spectrometer by analyzing their resistance to dissociation.[40] Native ESI-MS is highly sensitive and rapid and has a low sample consumption, making it a powerful structural biology technique. According to native ESI-MS analyses, FpvC and FpvF were purified in our experimental conditions without any siderophore or metal bound to them (Table 2). These analyses also demonstrated that FpvF can form dimers ($FpvF_2$), whereas FpvC did not (Table 2).

We next aimed to identify the compounds that bind to FpvC and FpvF and thus eventually transported by the FpvDE transporter. The purified periplasmic binding proteins FpvC and FpvF were individually incubated in the presence of 10 equiv of apo PVDI, PVDI-Fe, or siderophore-free Fe^{3+} before ESI-MS analyses (Table 2 and Figure 4). The molecular weights of PVDI (1336 Da) and PVDI-Fe (1388 Da) were checked by ESI-MS analysis. No interaction was observed between siderophore-free Fe^{3+} and either FpvC or FpvF. In the presence of apo PVDI or PVDI-Fe, the major FpvC form detected was siderophore-free protein. Lower amounts of FpvC-PVDI or FpvC-PVDI-Fe were also detected (Table 2 and Figure 4A). However, FpvC is important for iron acquisition by PVDI, since deletion of *fpvC* affected ^{55}Fe accumulation (around 30% inhibition, Supplemental Figure 2) as *fpvCDEF* mutation.

For FpvF, the presence of PVD seemed to activate the formation of FpvF dimers ($FpvF_2$) with a molecular weight of 60.2 kDa, and only the dimer was able to interact with metal-free PVDI or PVDI-Fe (Table 2, Figure 4B and C). No interaction was seen between FpvF monomers and any form of PVDI. The signal intensity of the multicharged ions corresponding to $FpvF_2$-PVDI and $FpvF_2$-PVDI-Fe was lower than the signal intensity of the FpvF dimer ions (Figure 4B).

In conclusion, FpvC, which was predicted to be a metal-binding protein, exists only as a monomer and cannot bind *in vitro* siderophore-free Fe^{3+}, though it can interact with PVDI-Fe. FpvF, which belongs according its sequence to the siderophore binding protein family, forms dimers able to interact with apo PVDI or PVDI-Fe. No interaction was observed with siderophore-free iron. According to the amount of protein-PVD-Fe complexes detected by ESI-MS, FpvF seems to be more efficient in interacting with PVDI-Fe than FpvC.

FpvC and FpvF Are Able To Interact and Form Two Complexes with Different Stoichiometries. When the purified periplasmic FpvC and FpvF proteins were incubated together in the absence of Fe^{3+} and siderophore, two complexes were observed by ESI-MS (Table 2 and Figure 5). The first complex comprised one FpvC and two FpvF proteins (FpvC-$FpvF_2$),

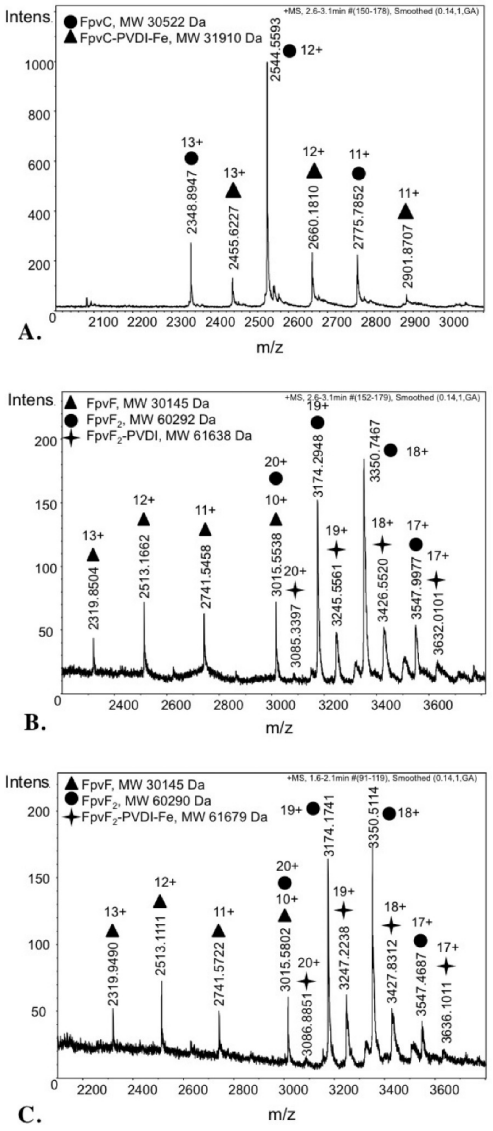

Figure 4. Native mass spectra of FpvC in the presence of PVDI-Fe (A) and of FpvF in the presence of PVDI-Fe (B) or apo PVDI (C). FpvC (A) and FpvF (B, C) were incubated independently, in the presence of 10 equiv of PVDI or PVDI-Fe in 100 mM ammonium acetate buffer pH 6.5. ESI-MS of the samples was performed under native conditions with final concentrations of FpvC and FpvF of 10 pmol/μL in 150 mM ammonium acetate. The capillary exit was 150 V for panels A and B and 160 V for panel C. The multicharged ions in panel A correspond to FpvC and FpvC-PVDI-Fe.

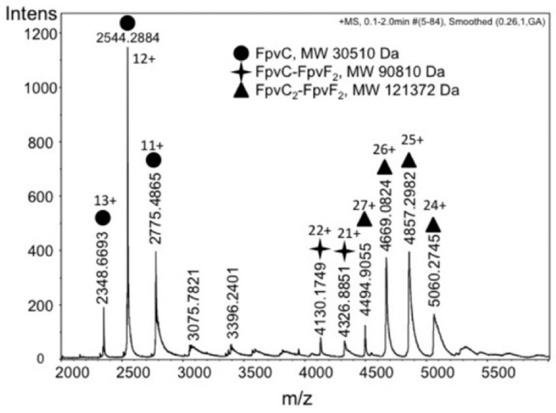

Figure 5. Native mass spectra of FpvC and FpvF incubated together. Equivalent amounts of FpvC and FpvF were incubated together in 100 mM ammonium acetate buffer pH 6.5. ESI-MS of the samples was performed under the same conditions as described in Figure 4.

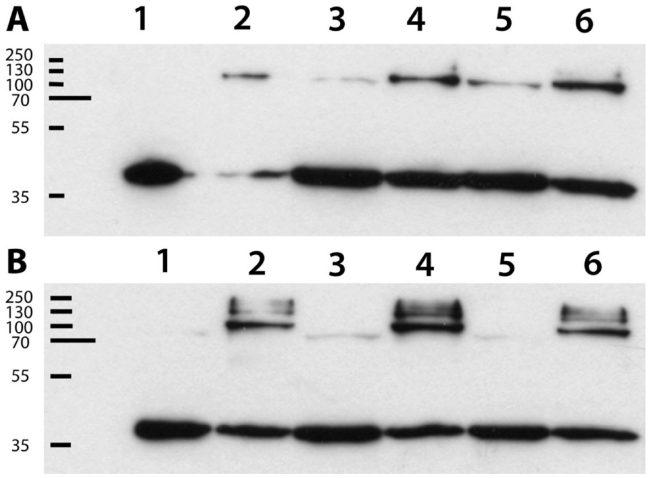

Figure 6. *In vivo* cross-linking of FpvC-FpvF complexes. PAO6382 grown in iron-limited medium were incubated in the presence of 1 μM PVDI-Fe or PVDI-Ga. After 30 min of incubation at room temperature, 1% formaldehyde was added, and the mixture incubated for another 30 min. Periplasmic proteins were isolated by cell fractionation, subjected to SDS-PAGE in a 12% polyacrylamide gel, and transferred to nitrocellulose membranes. FpvC (A) and FpvF (B) were detected with polyconal anti-FpvC and anti-FpvF. The cell were incubated without siderophore (lanes 1, 2), with 1 μM PVDI-Fe (lanes 3, 4), or with 1 μM PVDI-Ga (lanes 5, 6). In lanes 1, 3 and 5, the experiment has been performed in the absence of formaldehyde and in lanes 2, 4, and 6 with formaldehyde.

and the second complex was composed of dimers of both FpvC and FpvF ($FpvC_2$-$FpvF_2$). The ability of FpvC and FpvF to interact was confirmed *in vivo* with cross-linking experiments using formaldehyde (Figure 6). PAO6383 cells were incubated in the presence or absence of PVDI-Fe or PVDI-Ga and in the presence or absence of 1% formaldehyde. After incubation, the periplasmic proteins were isolated by cell fractionation and analyzed by SDS-PAGE. A new protein band was observed using polyclonal anti-FpvC and anti-FpvF at 110 kDa in the presence of formaldehyde as compared to the experiments in the absence of cross-linking agent, suggesting formation of FpvC-FpvF complexes *in vivo*. More FpvF has been observed in this cross-linking complex than FpvC suggesting a FpvC-$FpvF_2$ stoichiometry as observed by native mass spectrometry. At last, the amount of cross-linked FpvC-FpvF increased in the presence of PVDI-metal complexes, suggesting a stabilization of this protein complex in the presence of PVDI-Fe or PVDI-Ga.

FpvC-$FpvF_2$ and $FpvC_2$-$FpvF_2$ Complexes Are Able To Bind apo PVDI and PVDI-Fe. Purified FpvC and FpvF were incubated together in the presence of 10 or 20 equiv of apo PVDI, PVDI-Fe, or $FeCl_3$, and the interactions were followed by ESI-MS (Table 2 and Figure 7). Neither FpvC-$FpvF_2$ nor $FpvC_2$-$FpvF_2$ complexes interacted with siderophore-free iron. In the presence of 10 equiv of PVDI-Fe, complexes between FpvC, FpvF, and PVDI-Fe were observed. The stoichiometries of these complexes were 1:2:1:1, 1:2:2:2, 2:2:1:1, and 2:2:2:2 (FpvC:FpvF:PVDI:Fe; Figure 7A and Table 2), consistent with the molecular weights of the *in vivo* cross-link products in

dx.doi.org/10.1021/cb300330v | *ACS Chem. Biol.* 2012, 7, 2036–2045

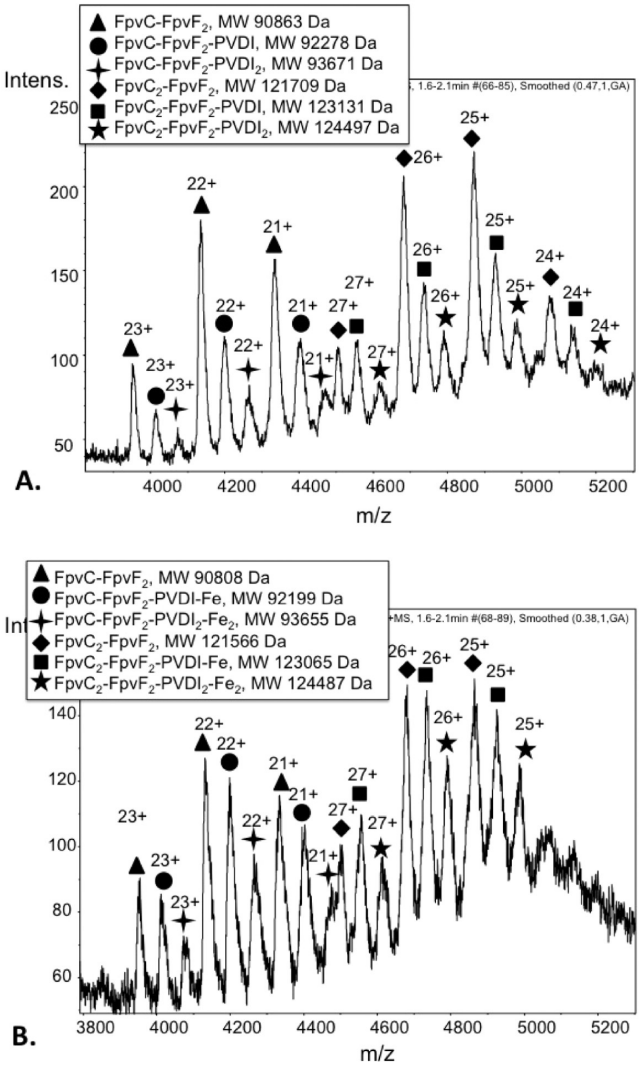

Figure 7. Native mass spectra of FpvC and FpvF incubated together in the presence of PVDI-Fe (A) or apo PVDI (B). FpvC and FpvF were incubated together, in the presence of 10 equiv of PVDI-Fe (A) or PVDI (B) in 100 mM ammonium acetate buffer pH 6.5. ESI-MS of the samples was performed under the same conditions as described in Figure 4.

Figure 6. The increase of PVDI-Fe concentration promoted the formation of large amounts of $FpvC_2$-$FpvF_2$-PVDI-Fe and $FpvC_2$-$FpvF_2$-$PVDI_2$-Fe_2 (data not shown). These data suggest that in the *P. aeruginosa* PVDI pathway, the ferrisiderophore in the periplasm interacts with FpvC-$FpvF_2$ and $FpvC_2$-$FpvF_2$ complexes and not just with one periplasmic binding protein. In the presence of PVDI-Ga, equivalent complexes were formed in the same proportions as with PVDI-Fe: FpvC-$FpvF_2$-PVDI-Ga, FpvC-$FpvF_2$-$PVDI_2$-Ga_2, $FpvC_2$-$FpvF_2$-PVDI-Ga, and $FpvC_2$-$FpvF_2$-$PVDI_2$-Ga_2 (Table 2 and Supplemental Figure 3).

When the experiment was repeated in the presence of apo PVDI, FpvC-FpvF-PVDI complexes were observed on ESI-MS with the following stoichiometries: 1:2:1, 1:2:2, 2:2:1, and 2:2:2 (Table 2 and Figure 7A).

The ability of FpvC-$FpvF_2$ and $FpvC_2$-$FpvF_2$ to bind both PVDI-Fe and apo PVDI, but not Fe^{3+}, suggests that these protein complexes interact more strongly with the PVDI moiety of PVDI-Fe and are thus present in the periplasm of *P. aeruginosa* cells to pick up PVDI-Fe after its transport across the outer membrane by FpvA. Consistent with this hypothesis, $FpvC_2$-$FpvF_2$ or FpvC-$FpvF_2$ were also able to interact with PVDI-Ga. At last and consistent with the *in vivo* cross-linking experiments, FpvC-$FpvF_2$ and $FpvC_2$-$FpvF_2$ complexes were more efficient in binding PVDI-Fe than the individual FpvC and FpvF proteins.

Conclusion. FpvCDEF is the first example of an ABC transporter with two associated periplasmic binding proteins involved in iron uptake by siderophores in Gram-negative bacteria. FpvC and FpvF are able to form complexes *in vivo* in the periplasm and bind PVDI-Fe. Previous approaches have shown that PVD-Fe, after uptake across the outer membrane by FpvA, dissociates in *P. aeruginosa* periplasm without any chemical modification of the siderophore but probably *via* a metal reduction step. In such a scenario and according to the data presented here, the two periplasmic FpvC and FpvF must pick up PVDI-Fe in the periplasm after transport by FpvA but do not bring the PVDI-Fe complex to the FpvE permease for uptake across the inner membrane. Instead, they must be somehow involved in the periplasmic dissociation of iron from PVDI and the subsequent transport of iron across the inner membrane into the cytoplasm by FpvDE. Deletion of the four genes of this ABC transporter did not completely inhibit Fe^{55} uptake by PVDI (Figure 2). This is probably because, even in the absence of FpvCDEF and therefore of the $FpvC_2$-$FpvF_2$ complex, FpvA is still functional. PVDI-^{55}Fe can thus accumulate in the periplasm as reported for PVDI-Ga and other PVDI-metal complexes that are unable to dissociate in *P. aeruginosa*.[41] PVDI-Fe dissociation was more dramatically affected by *fpvCDEF* deletion (Figure 3), indicating that this step must involve FpvC and FpvF. FpvC has three His and one Asp conserved amino-acid residues. We thus hypothesized that within the FpvC-$FpvF_2$-PVDI-Fe, FpvC-$FpvF_2$-$PVDI_2$-Fe_2, $FpvC_2$-$FpvF_2$-PVDI-Fe, and $FpvC_2$-$FpvF_2$-$PVDI_2$-Fe_2 complexes these four conserved residues are ready for an exchange with PVDI regarding the coordination of iron. Previous studies have shown that PVDI-Cr was unable to dissociate in the periplasm,[23] confirming that the dissociation mechanism must include a ligand exchange. Indeed, Cr forms complexes with siderophores that are structurally similar to siderophore-Fe but are inert to ligand exchange.[42] In such a scenario, where both FpvC and FpvF participate in the periplasmic dissociation of PVDI-Fe, there may be a dissociation mechanism where $FpvC_2$-$FpvF_2$-$PVDI_2$-Fe_2 dissociates into FpvC-Fe and FpvF-PVDI or $FpvC_2$-Fe_2 and $FpvF_2$-$PVDI_2$. In agreement with this notion, mass-spectrometry analyses clearly showed that FpvF was more efficient in binding apo PVDI than FpvC. However, neither FpvC nor FpvF was able to bind Fe^{3+} *in vitro*, although further investigations under anaerobic conditions are necessary to check whether FpvC can chelate Fe^{2+} instead of Fe^{3+}. Another next key step would consist in determining the X-ray structure of the $FpvC_2$-$FpvF_2$-$PVDI_2$-Fe_2 complex or to study the iron coordination in this complex.

METHODS

Chemicals, Growth Media, and Siderophores. $[^{55}Fe]Cl_3$ was obtained from PerkinElmer Life and Analytical Sciences (Boston, USA). The protonophore carbonyl cyanide *m*-chlorophenylhydrazone (CCCP) was purchased from Sigma, and isopropyl-D-1-thiogalactopyranoside (IPTG) was purchased from Euromedex.

P. aeruginosa PAO1 strains were grown overnight in succinate medium: 6.0 g L^{-1} K_2HPO_4, 3.0 g L^{-1} KH_2PO_4, 1.0 g L^{-1} $[NH_4]_2SO_4$, 0.2 g L^{-1} $MgSO_4{\cdot}7H_2O$, 4.0 g L^{-1} sodium succinate; the pH was adjusted to 7.0 by addition of NaOH at 30 °C. LB broth (Lennox)

and LB broth agar medium were both purchased from Difco and were used as rich medium in all experiments. Media were supplemented as necessary with the relevant antibiotics at the following concentrations: 50 μg mL^{-1} kanamycin, 100 μg mL^{-1} ampicillin, 150 μg mL^{-1} carbenicillin, 100 μg mL^{-1} tetracyclin, and 10 μg mL^{-1} chloramphenicol.

PVD and PVD-Fe were purified and prepared as previously described.[43]

Bacterial Strains and Plasmids. The strains and plasmids used in this study are summarized in Table 1. Mutation or cloning strategies are described in Supporting Information.

Iron Uptake Assays and Cell Fractionation. PVD-^{55}Fe (0.25 Ci mmol^{-1}) was prepared as previously described,[44] with a 4-fold excess of PVDI over iron. The uptake assays were carried out as previously described.[44] An overnight culture under conditions of iron limitation was performed. Bacteria were harvested and prepared in 50 mM Tris-HCl (pH 8.0) at an $OD_{600\ nm}$ of 1 and were incubated at 37 °C. Transport assays were initiated by adding 100 and 500 nM of PVDI-^{55}Fe. Aliquots (100 μL) of the suspension were removed at different times, filtered, and washed with 50 mM Tris-HCl, and the retained radioactivity was counted. The experiment was repeated with cells that had been previously treated with 200 μM CCCP, which is a protonophore that inhibits iron uptake.[36]

Periplasm and cytoplasm fractions were prepared as previously described.[45]

Fluorescence Spectroscopy. Fluorescence experiments were performed with a PTI (Photon Technology International TimeMaster; Bioritech) spectrofluorometer. The cells were washed with 2 vol of 50 mM Tris-HCl pH 8.0 and were then resuspended in the same buffer to a final $OD_{600\ nm}$ of 1. For all experiments, the sample was stirred at 29 °C in a 1 mL cuvette; the excitation wavelength was set at 400 nm, and fluorescence emission was measured at 447 nm, every 300 ms, for the duration of the experiment.

Expression and Protein Purification. *Expression and Purification of FpvC.* *E. coli* BL21 (DE3) carring pET23-789 were grown at 37 °C in Luria−Bertani (LB) medium containing 100 μg/mL ampicillin and 40 μM $FeSO_4$. After 24 h of culture, bacteria were harvested and resuspended in buffer A (50 mM Tris-HCl pH 8.0, 1 mM EDTA, 20% sucrose). To isolate the periplasmic fraction was added 1 mg mL^{-1} lysozyme, and the mixture was incubated for 2 min on ice. The suspension was then centrifuged for 20 min at 6,700*g*. The supernatant containing the periplasmic fraction was ultracentrifuged at 125,000*g* for 20 min to remove membrane traces from the sample. The periplasm was diluted 3X in a solution of 50 mM MES pH 6.5 and 1 mM EDTA, loaded onto a Source S column (GE Healthcare) equilibrated with 50 mM MES pH 6.5 and 1 mM EDTA, and then eluted with a linear gradient of 0−1 M NaCl. The fractions containing FpvC (as determined by SDS-PAGE) were pooled, concentrated, and placed onto a Superdex 200 10/300 GL column (GE Healthcare) equilibrated with 50 mM MES pH 6.5 and 350 mM NaCl. The fractions containing FpvC were loaded onto a HiTrap Desalting column (GE Healthcare) equilibrated with 50 mM MES pH 6.5 to remove salts from the sample. After purification, all of the protein fractions were pooled and concentrated by ultrafiltration at 10,000*g* using a molecular cutoff weight of 10 kDa (Amicon, Millipore).

Expression and Purification of FpvF. BL21(DE3) expressing FpvF were grown at 37 °C in LB medium with 100 μg mL^{-1} ampicillin until the cultured cells reached an OD_{600} of 0.6. Expression of the recombinant protein was induced with 1 mM IPTG at 37 °C for 3 h. Cells were harvested by centrifugation, resuspended in a solution of 50 mM Tris-HCl pH 8.0 and EDTA 1 mM, and then disrupted by two sonications (50−60% amplitude). Soluble proteins were separated from the cell membranes by a 125,000*g* ultracentrifugation for 20 min. Twenty millimolar imidazole was added to the supernatant containing FpvF. The sample was applied onto a HisTrap column (GE Healthcare) equilibrated in a solution containing 50 mM Tris-HCl pH 8.0, 500 mM NaCl, 20 mM imidazole. The protein was eluted with a linear gradient of 50 mM Tris-HCl pH 8.0, 500 mM NaCl, 500 mM imidazole. The fractions containing FpvF (as determined by SDS-PAGE) were pooled, concentrated, and washed by ultrafiltration with 50 mM Tris-HCl pH 7.5 and loaded onto a HiTrap Q column equilibrated with 50 mM Tris-HCl pH 7.5. The protein was eluted with a linear gradient of 0−1 M NaCl in 50 mM Tris-HCl pH 7.5. The FpvF fractions were loaded onto a HiTrap desalting column (GE Healthcare) equilibrated with 50 mM Tris-HCl pH 7.5 to remove salt traces from the sample. After purification, all of the protein fractions were then pooled and concentrated by ultrafiltration at 10,000*g* using a molecular cutoff weight of 10 kDa (Amicon, Millipore).

Electrospray Mass Spectrometry Analysis. All studies were performed using an electrospray time-of-flight mass spectrometer (ESI-MS) (MicrOTOF II, Bruker, Bremen, Germany). The FpvC and FpvF proteins were prepared at 100 μM concentration in 100 mM ammonium acetate buffer pH 6.5. Ultrafiltration at 10,000*g* using a molecular cutoff weight of 10 kDa (Amicon, Millipore) was used for the buffer exchange. Proteins were incubated with the equivalent of 10−20 $FeCl_3$, PVDI, or PVDI-Fe. Samples were analyzed under denaturing conditions at a final concentration of 5 pmol μL^{-1} in water/acetonitrile v/v 1% formic acid and under native conditions at a final concentration of 10 pmol μL^{-1} in 150 mM ammonium acetate. The samples were continuously infused into the ion source at a flow rate of 3 μL min^{-1} using a syringe pump (KD Scientific, Holliston, MA, USA). Data were acquired in the positive mode. An ESI-L low-concentration tuning mix (Agilent Technologies) was used to calibrate the device for denaturation analyses, whereas a 1 mg mL^{-1} solution of cesium iodide (Fluka) in ethanol was used to calibrate the device for native analyses. To preserve the noncovalent complexes, relatively mild interface conditions were used; a declustering voltage (Capillary exit) was ranged from 40 to 200 V, and the capillary temperature was set to 160 and 180 °C. The time of acquisition was between 30 s and 1 min. Data were analyzed with Data Analysis software (ver 4.0 SP1, Bruker) and the protein electro-spray spectra were deconvoluted using Maximum Entropy or Charge State Ruler.

Cross-Linking. An overnight culture of PAO6383 (50 mL) in iron-limited medium was harvested and washed twice in 50 mM sodium phosphate buffer (pH 6.8). The cell suspension was incubated in the presence of 1 μM PVDI-Fe or 1 μM PVDI-Ga during 30 min. After incubation at RT, the cells were incubated another 30 min in the presence or absence of 1% formaldehyde. The cells were harvested and resuspended in 50 mM Tris-HCl (pH 8.0), 1 mM EDTA, and 20% sucrose to isolate the periplasmic fractions as described above. The periplamic fractions were analyzed by immunoblotting using FpvC and FpvF antibodies.

Immunoblot Analysis. Proteins were transferred onto nitrocellulose membranes by electroblotting (Bio-Rad). The nitrocellulose membranes were then blocked by incubation for 20 min in phosphate-buffered saline (PBS, pH 7.6, 5% dried milk powder) followed by incubation in blocking buffer supplemented with a primary antibody. They were then incubated in blocking buffer supplemented with a peroxidase-conjugated goat anti-rabbit IgG secondary antibody (Sigma, dilution 1/10000). Antibody binding was detected by enhanced chemiluminescence (SuperSignal West Pico Chemiluminescent Subtrate, Pierce). Anti-FpvC and anti-FpvF polyclonal antisera were prepared from purified FpvC and FpvF, respectively. New Zealand rabbits were immunized with 200 μg of proteins in 1 mL of PBS and Freund's Complete Adjuvant V.

■ ASSOCIATED CONTENT

Supporting Information

This material is available free of charge *via* the Internet at http://pubs.acs.org.

■ AUTHOR INFORMATION

Corresponding Author

*E-mail: isabelle.schalk@unistra.fr.

Notes

The authors declare no competing financial interest.

■ ACKNOWLEDGMENTS

This work was partly funded by the Centre National de la Recherche Scientifique and by grants from the Centre International de Recherche au Frontière de la Chimie (FRC) and from the ANR (Agence Nationale de Recherche, ANR-08-BLAN-0315-01). We thank B. Hass and A. Chapelle for their help in the construction of pVEGA6 and pET23-789 vectors, respectively.

■ REFERENCES

(1) Meyer, J. M., Geoffroy, V. A., Baida, N., Gardan, L., Izard, D., Lemanceau, P., Achouak, W., and Palleroni, N. J. (2002) Siderophore typing, a powerful tool for the identification of fluorescent and nonfluorescent *pseudomonads*. *Appl. Environ. Microbiol. 68*, 2745–2753.

(2) Hider, R. C., and Kong, X. (2011) Chemistry and biology of siderophores. *Nat. Prod. Rep. 27*, 637–657.

(3) Ratledge, C., and Dover, L. G. (2000) Iron metabolism in pathogenic bacteria. *Annu. Rev. Microbiol. 54*, 881–941.

(4) Meyer, J. M., Gruffaz, C., Raharinosy, V., Bezverbnaya, I., Schafer, M., and Budzikiewicz, H. (2008) Siderotyping of fluorescent *Pseudomonas*: molecular mass determination by mass spectrometry as a powerful pyoverdine siderotyping method. *Biometals 21*, 259–271.

(5) Demange, P., Wendenbaum, S., Linget, C., Mertz, C., Cung, M. T., Dell, A., and Abdallah, M. A. (1990) Bacterial siderophores: structure and NMR assigment of pyoverdins PaA, siderophores of *Pseudomonas aeruginosa* ATCC 15692. *Biol. Metals 3*, 155–170.

(6) Poole, K., and McKay, G. A. (2003) Iron acquisition and its control in *Pseudomonas aeruginosa*: many roads lead to Rome. *Front. Biosci. 8*, d661–686.

(7) Brillet, K., Journet, L., Celia, H., Paulus, L., Stahl, A., Pattus, F., and Cobessi, D. (2007) A β-strand lock-exchange for signal transduction in TonB-dependent transducers on the basis of a common structural motif. *Structure 15*, 1383–1391.

(8) Wirth, C., Meyer-Klaucke, W., Pattus, F., and Cobessi, D. (2007) From the periplasmic signaling domain to the extracellular face of an outer membrane signal transducer of *Pseudomonas aeruginosa*: crystal structure of the ferric pyoverdine outer membrane receptor. *J. Mol. Biol. 68*, 398–406.

(9) Schalk, I. J., Lamont, I. L., and Cobessi, D. (2009) Structure-function relationships in the bifunctional ferrisiderophore FpvA receptor from *Pseudomonas aeruginosa*. *Biometals 22*, 671–678.

(10) Adams, H., Zeder-Lutz, G., Greenwald, J., Schalk, I. J., Célia, H., and Pattus, F. (2006) Interaction of TonB with outer membrane receptor FpvA of *Pseudomonas aeruginosa*. *J. Bacteriol. 188*, 5752–5761.

(11) Zhao, Q., and Poole, K. (2002) Mutational analysis of the TonB1 energy coupler of *Pseudomonas aeruginosa*. *J. Bacteriol. 184*, 1503–1513.

(12) Koster, W. (2001) ABC transporter-mediated uptake of iron, siderophores, heme and vitamin B12. *Res. Microbiol. 152*, 291–301.

(13) Cuiv, P. O., Clarke, P., Lynch, D., and O'Connell, M. (2004) Identification of *rhtX* and *fptX*, novel genes encoding proteins that show homology and function in the utilization of the siderophores rhizobactin 1021 by *Sinorhizobium meliloti* and pyochelin by *Pseudomonas aeruginosa*, respectively. *J. Bacteriol. 186*, 2996–3005.

(14) Hannauer, M., Barda, Y., Mislin, G. L., Shanzer, A., and Schalk, I. J. (2010) The ferrichrome uptake pathway in *Pseudomonas aeruginosa* involves an iron release mechansim with acylation of the siderophore and a recycling of the modified desferrichrome. *J. Bacteriol. 192*, 1212–1220.

(15) Koster, W., and Braun, V. (1986) Iron hydroxamate transport of *Escherichia coli*: nucleotide sequence of the *fhuB* gene and identification of the protein. *Mol. Gen. Genet. 204*, 435–442.

(16) Koster, W., and Braun, V. (1989) Iron-hydroxamate transport into *Escherichia coli* K12: localization of FhuD in the periplasm and of FhuB in the cytoplasmic membrane. *Mol. Gen. Genet. 217*, 233–239.

(17) Braun, V., and Herrmann, C. (2007) Docking of the periplasmic FecB binding protein to the FecCD transmembrane proteins in the ferric citrate transport system of *Escherichia coli*. *J. Bacteriol. 189*, 6913–6918.

(18) Staudenmaier, H., Van Hove, B., Yaraghi, Z., and Braun, V. (1989) Nucleotide sequences of the *fecBCDE* genes and locations of the proteins suggest a periplasmic-binding-protein-dependent transport mechanism for iron(III) dicitrate in *Escherichia coli*. *J. Bacteriol. 171*, 2626–2633.

(19) Chenault, S. S., and Earhart, C. F. (1991) Organization of genes encoding membrane proteins of the *Escherichia coli* ferrienterobactin permease. *Mol. Microbiol. 5*, 1405–1413.

(20) Matzanke, B. F., Anemuller, S., Schunemann, V., Trautwein, A. X., and Hantke, K. (2004) FhuF, part of a siderophore-reductase system. *Biochemistry 43*, 1386–1392.

(21) Hartman, A., and Braun, V. (1980) Iron transport in *Escherichia coli*: uptake and modification of ferrichrome. *J. Bacteriol. 143*, 246–255.

(22) Brickman, T. J., and McIntosh, M. A. (1992) Overexpression and purification of ferric enterobactin esterase from *Escherichia coli*. Demonstration of enzymatic hydrolysis of enterobactin and its iron complex. *J. Biol. Chem. 267*, 12350–12355.

(23) Greenwald, J., Hoegy, F., Nader, M., Journet, L., Mislin, G. L. A., Graumann, P. L., and Schalk, I. J. (2007) Real-time FRET visualization of ferric-pyoverdine uptake in *Pseudomonas aeruginosa*: a role for ferrous iron. *J. Biol. Chem. 282*, 2987–2995.

(24) Yeterian, E., Martin, L. W., Lamont, I. L., and Schalk, I. J. (2010) An efflux pump is required for siderophore recycling by *Pseudomonas aeruginosa*. *Environ Microbiol Report 2*, 412–418.

(25) Imperi, F., Tiburzi, F., and Visca, P. (2009) Molecular basis of pyoverdine siderophore recycling in *Pseudomonas aeruginosa*. *Proc. Natl. Acad. Sci. U. S. A. 106*, 20440–20445.

(26) Schalk, I. J., Abdallah, M. A., and Pattus, F. (2002) Recycling of pyoverdin on the FpvA receptor after ferric pyoverdin uptake and dissociation in *Pseudomonas aeruginosa*. *Biochemistry 41*, 1663–1671.

(27) Ravel, J., and Cornelis, P. (2003) Genomics of pyoverdine-mediated iron uptake in *pseudomonads*. *Trends Microbiol. 11*, 195–200.

(28) Llamas, M. A., Mooij, M. J., Sparrius, M., Vandenbroucke-Grauls, C. M., Ratledge, C., and Bitter, W. (2008) Characterization of five novel *Pseudomonas aeruginosa* cell-surface signalling systems. *Mol. Microbiol. 67*, 458–472.

(29) Ochsner, U., Snyder, A., Vasil, A. I., and Vasil, M. L. (2002) Effects of the twin-arginine translocase on secretion of virulence factors, stress response, and pathogenesis. *Proc. Natl. Acad. Sci. U.S.A. 99*, 8312–8317.

(30) Ochsner, U. A., Wilderman, P. J., Vasil, A. I., and Vasil, M. L. (2002) GeneChip expression analysis of the iron starvation response in *Pseudomonas aeruginosa*: identification of novel pyoverdine biosynthesis genes. *Mol. Microbiol. 45*, 1277–1287.

(31) Llamas, M. A., Sparrius, M., Kloet, R., Jimenez, C. R., Vandenbroucke-Grauls, C., and Bitter, W. (2006) The heterologous siderophores ferrioxamine B and ferrichrome activate signaling pathways in *Pseudomonas aeruginosa*. *J. Bacteriol. 188*, 1882–1891.

(32) Lee, Y. H., Deka, R. K., Norgard, M. V., Radolf, J. D., Hasemann, C. A., Journet, L., Bouveret, E., Rigal, A., Lloubes, R., Lazdunski, C., Benedetti, H., Larsen, R. A., Thomas, M. G., and Postle, K. (1999) Treponema pallidum TroA is a periplasmic zinc-binding protein with a helical backbone. *Nat. Struct. Biol. 6*, 628–633.

(33) Berntsson, R. P., Smits, S. H., Schmitt, L., Slotboom, D. J., and Poolman, B. (2010) A structural classification of substrate-binding proteins. *FEBS Lett. 584*, 2606–2617.

(34) Bendtsen, J. D., Nielsen, H., von Heijne, G., and Brunak, S. (2004) Improved prediction of signal peptides: SignalP 3.0. *J. Mol. Biol. 340*, 783–795.

(35) Chu, B. C., and Vogel, H. J. (2011) A structural and functional analysis of type III periplasmic and substrate binding proteins: their role in bacterial siderophore and heme transport. *Biol. Chem. 392*, 39–52.

(36) Clément, E., Mesini, P. J., Pattus, F., Abdallah, M. A., and Schalk, I. J. (2004) The binding mechanism of pyoverdin with the outer

membrane receptor FpvA in *Pseudomonas aeruginosa* is dependent on its iron-loaded status. *Biochemistry 43*, 7954−7965.
(37) Folschweiller, N., Gallay, J., Vincent, M., Abdallah, M. A., Pattus, F., and Schalk, I. J. (2002) The interaction between pyoverdin and its outer membrane receptor in *Pseudomonas aeruginosa* leads to different conformers: a time-resolved fluorescence study. *Biochemistry 41*, 14591−14601.
(38) Schalk, I. J., Kyslik, P., Prome, D., van Dorsselaer, A., Poole, K., Abdallah, M. A., and Pattus, F. (1999) Copurification of the FpvA ferric pyoverdin receptor of *Pseudomonas aeruginosa* with its iron-free ligand: implications for siderophore-mediated iron transport. *Biochemistry 38*, 9357−9365.
(39) Xiao, R., and Kisaalita, W. S. (1998) Fluorescent pseudomonad pyoverdines bind and oxidize ferrous ion. *Appl. Environ. Microbiol. 64*, 1472−1476.
(40) Loo, J. A. (1997) Studying noncovalent protein complexes by electrospray ionization mass spectrometry. *Mass Spectrom. Rev. 16*, 1−23.
(41) Schalk, I. J., Hannauer, M., and Braud, A. (2011) New roles for bacterial siderophores in metal transport and tolerance. *Environ. Microbiol. 13*, 2844−2854.
(42) Leong, J., and Neilands, J. B. (1976) Mechanisms of siderophore iron transport in enteric bacteria. *J. Bacteriol. 126*, 823−830.
(43) Albrecht-Gary, A. M., Blanc, S., Rochel, N., Ocacktan, A. Z., and Abdallah, M. A. (1994) Bacterial iron transport: coordination properties of pyoverdin PaA, a peptidic siderophore of *Pseudomonas aeruginosa*. *Inorg. Chem. 33*, 6391−6402.
(44) Schalk, I. J., Hennard, C., Dugave, C., Poole, K., Abdallah, M. A., and Pattus, F. (2001) Iron-free pyoverdin binds to its outer membrane receptor FpvA in *Pseudomonas aeruginosa*: a new mechanism for membrane iron transport. *Mol. Microbiol. 39*, 351−360.
(45) Nader, M., Journet, L., Meksem, A., Guillon, L., and Schalk, I. J. (2011) Mechanism of ferrisiderophore uptake by *Pseudomonas aeruginosa* outer membrane transporter FpvA: no diffusion channel formed at any time during ferrisiderophore uptake. *Biochemistry 50*, 2530−2540.
(46) Stover, C. K., Pham, X. Q., Erwin, A. L., Mizoguchi, S. D., Warrener, P., Hickey, M. J., Brinkman, F. S., Hufnagle, W. O., Kowalik, D. J., Lagrou, M., Garber, R. L., Goltry, L., Tolentino, E., Westbrock-Wadman, S., Yuan, Y., Brody, L. L., Coulter, S. N., Folger, K. R., Kas, A., Larbig, K., Lim, R., Smith, K., Spencer, D., Wong, G. K., Wu, Z., Paulsen, I. T., Reizer, J., Saier, M. H., Hancock, R. E., Lory, S., and Olson, M. V. (2000) Complete genome sequence of *Pseudomonas aeruginosa* PAO1, an opportunistic pathogen. *Nature 406*, 959−964.
(47) Hoegy, F., Lee, X., Noël, S., Mislin, G. L., Rognan, D., Reimmann, C., and Schalk, I. J. (2009) Stereospecificity of the siderophore pyochelin outer membrane transporters in fluorescent *Pseudomonads*. *J. Biol. Chem. 284*, 14949−14957.
(48) Shirley, M., and Lamont, I. L. (2009) Role of TonB1 in pyoverdine-mediated signaling in *Pseudomonas aeruginosa*. *J. Bacteriol. 191*, 5634−5640.
(49) Morales, V. M., Backman, A., and Bagdasarian, M. (1991) A series of wide-host-range low-copy-number vectors that allow direct screening for recombinants. *Gene 97*, 39−47.
(50) Voisard, C., Bull, C., Keel, C., Laville, J., Maurhofer, M., Schnider, U., Défago, G., Haas, D. (1994) Biocontrol of root diseases by *Pseudomonas fluorescens* CHAO: current concepts and experimental approaches, in *Molecular Ecology of Rhizosphere Microorganisms* (O'Gara, F., Dowling, D. N., and Boesten, B., Eds.), pp 67−89, VCH, Weinheim, Germany.
(51) Blumer, C., Heeb, S., Pessi, G., and Haas, D. (1999) Global GacA-steered control of cyanide and exoprotease production in *Pseudomonas fluorescens* involves specific ribosome binding sites. *Proc. Natl. Acad. Sci. U.S.A. 96*, 14073−14078.
(52) Larkin, M. A., Blackshields, G., Brown, N. P., Chenna, R., McGettigan, P. A., McWilliam, H., Valentin, F., Wallace, I. M., Wilm, A., Lopez, R., Thompson, J. D., Gibson, T. J., and Higgins, D. G. (2007) Clustal W and Clustal X version 2.0. *Bioinformatics 23*, 2947−2948.